
Inversion of Simulated Positron Annihilation Lifetime Spectra by Moving Boundary Subspaces

V. C. VITERBO,¹ J. L. NEVES,¹ J. P. BRAGA,¹ R. P. G. MONTEIRO,²
W. F. DE MAGALHÃES¹

¹Departamento de Química—ICEx, Universidade Federal de Minas Gerais, 31270-901 Belo Horizonte, Minas Gerais, Brasil

²CNEN—Centro de Desenvolvimento da Tecnologia Nuclear, Minas Gerais, Brasil

Received 17 November 2001; accepted 16 April 2003

DOI 10.1002/qua.10658

ABSTRACT: The retrieval of the density function for the positron annihilation lifetime spectrum is obtained from simulated data using the damped singular value decomposition. Two filter factors were discussed, for noise and noiseless data, and under the L curve criterion. The obtained density function is exact in the absence of noise. When noise is considered, the predicted peaks are at positions $\lambda_1 = 0.4167 \text{ ns}^{-1}$, $\lambda_2 = 2.418 \text{ ns}^{-1}$, whereas the exact results are $\lambda_1 = 0.5250 \text{ ns}^{-1}$ and $\lambda_2 = 2.538 \text{ ns}^{-1}$. The computed areas for these peaks are also in fair agreement when compared with the theoretical results. In this case, a filter factor that takes into account all the singular values was found appropriate. The current study shows that the damped singular value decomposition approach can be used to invert real laboratory data. © 2003 Wiley Periodicals, Inc. *Int J Quantum Chem* 95: 97–102, 2003

Key words: ill-posed; inversion; positron annihilation; singular value decomposition

Introduction

The counting of photons as a function of time, from a positron annihilation process, can give important information about the medium under consideration. The positrons, usually from a ^{22}Na

source, while traveling through the medium can collide with the molecules, and several processes can occur [1]. The free positron can get solvated to later on, annihilate to two photons ($2 - \gamma$) at about 0.4 ns. It can also, with an electron, form the positronium (P_s), either in its singlet state—the para- $P_s(p - P_s)$ —or the triplet state, ortho $P_s(o - P_s)$. The intrinsic annihilation of the $p - P_s$, in a $2 - \gamma$ process, happens at about 0.13 ns. This $2 - \gamma$ process can also occur with the triplet state at about $1 -$

Correspondence to: J. P. Braga; e-mail: jpbbraga@oxigenio. qui.ufmg.br

Contract grant sponsors: CNPq; FAPEMIG.

5 ns, although the $o - Ps$ must combine with another electron (pick-off annihilation).

The inversion of the above positron annihilation process, to obtain the positron lifetime spectrum [2], can be represented as a Fredholm integral equation of first kind [3], which here will be represented in the discret form $\mathbf{K}\mathbf{f} = \mathbf{c}$. The calculation of the density function, $f(\lambda)$, λ being the annihilation rate, is represented by \mathbf{f} and is especially important for the experimentalist because it can give information about the properties of the medium. In the above representation, the matrix \mathbf{K} represents the kernel of the integral equation, $K(t, \lambda) = e^{-\lambda t}$ and \mathbf{c} , the counting of positron annihilation, $c(t)$.

The current inversion is considered an ill-posed problem, that is, a problem that is defined whenever one of the three conditions—existence, uniqueness, or continuity—is not fulfilled [4]. The representation of the above kernel, together with the experimental errors in the data, is sufficient to classify this problem as ill-posed. Due to the character of the kernel, errors are largely amplified when the inverse problem is to be solved.

Several methods are available to handle ill-posed problems [4], the most common being the Tikhonov regularization [5, 6]; the singular value decomposition [7], also known as the moving boundary subspaces; and neural network [8]. These methods have been applied to invert thermodynamic data [9, 10] and simulated positron annihilation lifetime spectra [11] where no noises were taken into account. In the current work, the inversion of simulated positron lifetime spectra, with and without noise, is investigated using the moving boundary subspaces method for two filter factors and under the L curve criterion. The effect of noise in the simulated data can be used as a preliminary study to invert real laboratory data.

Theoretical Background

An essential step while calculating the probability density function is to understand the subspace structure of the data and the solution. The two methods to be used for this purpose, the singular value decomposition and the Tikhonov, have an adjustable parameter to be determined on physical grounds. In the singular value decomposition this parameter is related to the dimension of the subspaces and in this case the method is also called the moving boundary subspace method. For the Tik-

honov regularization, it is related to a compromise between residual and solution norms.

For a representation with n points and m data, that is, $\mathbf{K} \in R^{m \times n}$, $\mathbf{f} \in R^n$ and $\mathbf{c} \in R^m$, the problem can be considered as a linear transformation between the spaces R^n and R^m , which can be divided into two subspaces. One of these subspaces is the range of \mathbf{K} , denoted by $R(\mathbf{K})$. If \mathbf{f} does not belong to this subspace, the solution of the problem can be only approximate. The uniqueness of the solution is related to another subspace, the nullspace of \mathbf{K} , $N(\mathbf{K})$. If this is a nonempty subspace, multiple solutions of the problem appear, preventing traditional inversion matrix algorithm from being used in the search for the solution of the problem. The two remaining subspaces, also one each in R^n and R^m , are analogous to the range and nullspace, defined for the transposition of the kernel representation.

The factorization of \mathbf{K} into $\mathbf{U}\Sigma\mathbf{V}^T$, \mathbf{U} , and \mathbf{V} being orthonormal and Σ diagonal matrices is the basic step to establish the four subspaces. Under this factorization [12], the density function can be written as

$$\mathbf{f}_s = \sum_{j=1}^k \frac{\mathbf{u}_j^T \cdot \mathbf{c}}{\sigma_j} \mathbf{v}_j \quad (1)$$

where \mathbf{u}_j and \mathbf{v}_j are the vectors column of \mathbf{U} and \mathbf{V} , and σ_j are the diagonal elements of Σ . The numerical calculation of the factorization plus the determination of the optimal value of k , the rank of the transformation, constitute the steps necessary to determine the solution of the problem.

Positron Annihilation Lifetime Spectra Model

The model system to study the inversion of positronium annihilation data is the same as that used before to invert data using neural network and given in Refs. [11] and [13].

The density function, from which the inversion is to be tested, was found in the form,

$$f(\lambda) = a_1 e^{-\alpha_1(\ln(\lambda) - \sigma_1)^2} + a_2 e^{-\alpha_2(\ln(\lambda) - \sigma_2)^2}. \quad (2)$$

The constants a_i , α_i , σ_i ($i = 1, 2$), were chosen to reproduce the positron annihilation data of lyso-

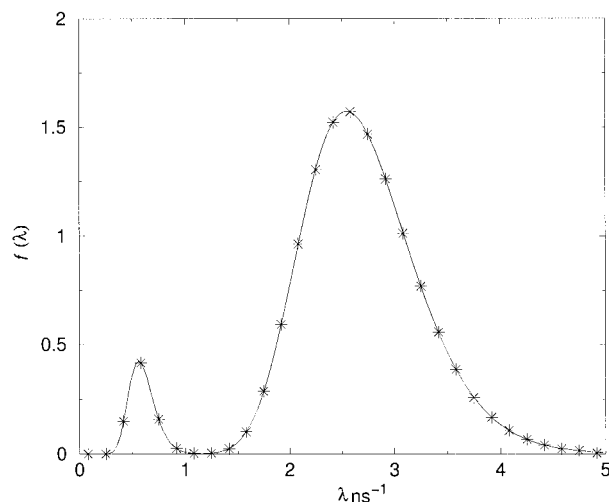


FIGURE 1. Inverted density function for the filter (4) and noiseless data. The solid line represents exact results, whereas the asterisks (*) represents computed results.

zome in water [13]. The constants are [11]: $a_1 = 0.42250$, $a_2 = 1.57270$, $\alpha_1 = 11.6951$, $\alpha_2 = 12.0688$, $\sigma_1 = -0.57710$, and $\sigma_2 = 0.93530$. From this density function the direct problem, that is, $\mathbf{c} = \mathbf{Kf}$, was established. This is used, as a reference, to understand the results from the moving boundary method. The theoretical results, \mathbf{c} and \mathbf{K} , are presented with this work, but four quantities are important for its characterization: the position, λ , and areas, A , of the peaks in the density function. The first peak in Eq. (2) happens at $\lambda_1 = 0.5250 \text{ ns}^{-1}$ with $A_1 = 5.684\%$ and may be attributed to the $o - Ps$ annihilation. The second peak, due to the free positron and $p - Ps$ annihilations, has $\lambda_2 = 2.538 \text{ ns}^{-1}$ and $A_2 = 94.32\%$. These four quantities are used when comparing the inverted results using the moving boundary method.

Density Function with Noiseless Data

The dimension of the spaces in which the data are to be represented is the first step in carrying out the inversion procedure. For $m = 30$, a residual error $\|\mathbf{Kf} - \mathbf{c}\|_2^2 = 7.884 \times 10^{-4}$ was found, implying this basis set dimension represents adequately the data. Nevertheless, in this case, $\dim N(\mathbf{K}) = 13$, characterizing the multiple solution of the problem. In fact, because the nullspace is nonempty, any solution can be written as a linear combination of a

solution belonging to the range and a solution belonging to the nullspace.

The density function was calculated for increasing dimensions of the range subspace. As k is increased, the residual error of the computed solution decreases. For $k < \text{rank}(\mathbf{K})$ unphysical results are obtained for the computed solution. The computed density function, for $k = \text{rank}(\mathbf{K}) = 17$, is presented in Figure 1. An excellent agreement with the expected results is obtained. For example, the left and right theoretical maximum occurs at 0.5250 ns^{-1} and 2.538 ns^{-1} , respectively. The singular value decomposition gives for these peaks 0.5833 ns^{-1} and 2.583 ns^{-1} . The area under each peak is also in excellent agreement. The first and second theoretical areas are 5.684% and 94.32% , whereas the computed values are 5.684% and 94.32% .

Retrieving the Density Function in the Presence of Noise Data

The above excellent results are not meant to imply that the method can be applied to experimental data. In this case, there is experimental noise that must be taken into consideration. To test the stability of the method in the presence of noise, a background noise, which follows the Poisson distribution, was added to the simulated counting.

The moving boundary subspaces method is very sensitive to errors introduced in the data. This is

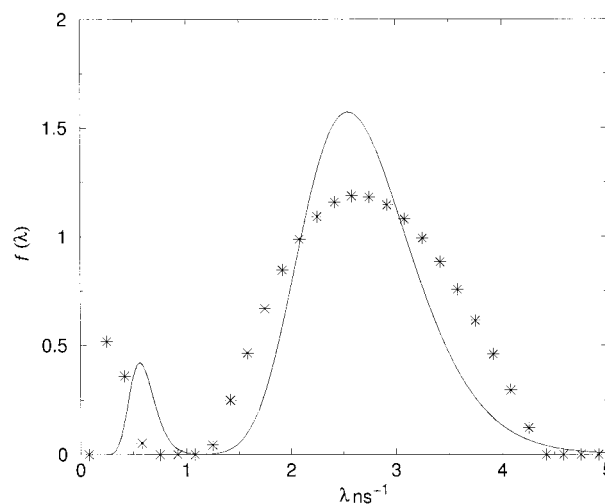


FIGURE 2. Calculated $f(\lambda)$ for noise data. The solid line represents exact results, whereas the asterisks (*) represent computed results.

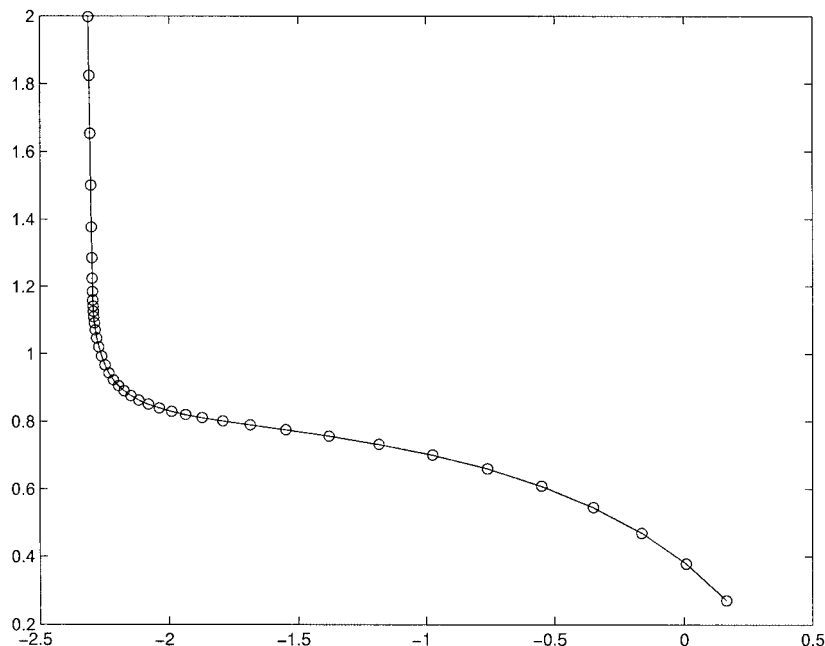


FIGURE 3. Optimal determination of η using the L curve.

clear when the exact counting is substituted by the noise data, $\mathbf{c} + \delta\mathbf{c}$, in the singular value decomposition solution. The change in the solution, $\delta\mathbf{f}_S = \mathbf{f}_{S,noise} - \mathbf{f}_S$, is given by

$$\delta\mathbf{f}_S = \sum_{j=1}^k \frac{\mathbf{u}_j^T \cdot \delta\mathbf{c}}{\sigma_j} \mathbf{v}_j. \quad (3)$$

Because the singular values go smoothly to zero, any small change in the data can make the solution diverge. The size of the four basic subspaces have to be redefined in the presence of noise.

The combination of the oscillating character of the basis set defined by the decomposition and the addition of noise makes the solution have nonphysical results, that is, the $f(\lambda)$ can assume, for some values of half-life, negative values. Consequently, additional restriction must be imposed on the problem. The restriction, $f(\lambda) = f(\lambda)$ if $f(\lambda) \geq 0$ and $f(\lambda) = 0$ elsewhere, also used in inversion problems in imaging [14] is then introduced into the solution from Eq. (1). The new result is shown in Figure 2. The simulated results for the half-life and areas are: $\lambda_1 = 0.2500 \text{ ns}^{-1}$, $\lambda_2 = 2.583 \text{ ns}^{-1}$, $A_1 = 6.150\%$, and $A_2 = 93.85\%$. Although the areas and the position of second peak are in good agreement with expected

results, there is also a possibility of changing the filter factor in the moving boundary method.

When defining the sizes of subspaces in previous results, the filter factor used was

$$g(i) = \begin{cases} 1 & i \leq k \\ 0 & i > k, \end{cases} \quad (4)$$

because the expansion (1) is truncated after some optimal value. This filter factor has the inconvenience of eliminating any contribution after some value of k while retrieving the density function. Instead, when a smooth filter factor is used, these neglected terms may be taken into consideration. For a restriction not only on the residual norm but also on the norm of the solution, that is, the filter for the Tikhonov regularization, one can write,

$$g(i) = \frac{\sigma_i^2}{\sigma_i^2 + \eta}. \quad (5)$$

The parameter η controls the importance of the residual and solution norms and has to be calculated. An appropriate way for its determination is to use the empirical L curve [4, 15]. These two norms were calculated for various values of this free parameter, the optimal value, η^* was calculated as a value close to

the corner of this "L-shaped" curve, as represented in Figure 3. This point has an important meaning: it is the point at which both, residual and solution norms, are appropriately weighted.

The optimal value of η was determined, giving $\eta^* = 9.6207 \times 10^{-6}$. This also establishes the filter factor (5), which is represented in Figure 4. The smooth character of this filter is clear from this figure. The inverted density function, with this new filter factor, is presented in Figure 5. The results for the peaks position and areas are: $\lambda_1 = 0.4167 \text{ ns}^{-1}$, $\lambda_2 = 2.418 \text{ ns}^{-1}$, $A_1 = 7.078\%$, and $A_2 = 92.92\%$, clearly showing overall improvement in the computed solution.

Conclusion

Density function calculation, in the positron annihilation process, was carried out by the moving boundary subspace method. For simulated data, in absence of noise, the recovering of this quantity was almost exact. The results are of comparable accuracy to those obtained by neural network [11].

Nevertheless, the above situation does not represent a real situation, and noise was included to simulate experimental data. In the presence of noise, the boundary of the subspaces have to be redefined as a consequence of error amplification. The first strategy adopted was to impose the condition $f(\lambda) \geq 0$, after a solution had been found. In the second alternative used, one seeks not only the

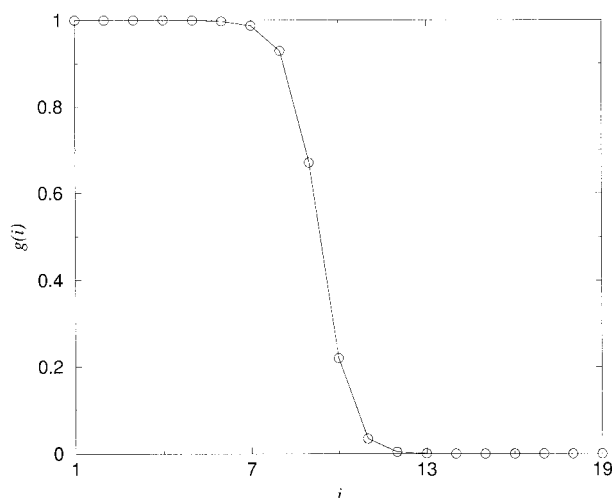


FIGURE 4. Filter factor (5) for the optimal value of η .

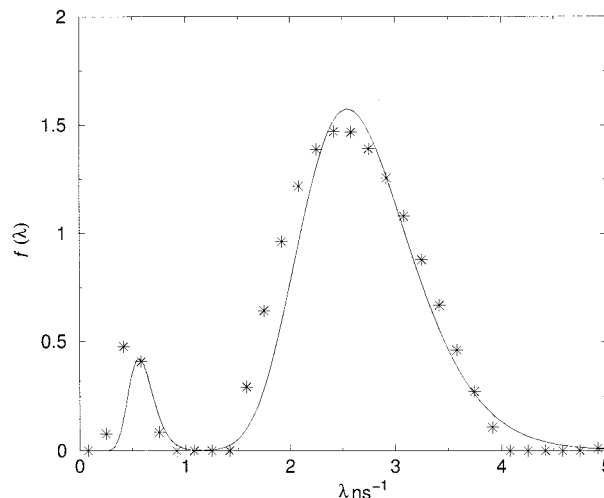


FIGURE 5. Inverted density function for the filter $g(i) = \sigma_i^2 / (\sigma_i^2 + \eta)$ and noise data. The solid line represents exact results, whereas the asterisks (*) represent computed results.

residual norm but also the solution norm. The extra parameter introduced in this case was determined by the L curve criterion.

Useful information about the structure of the density function can be obtained by the moving boundary subspace method. The positions and areas were recovered with tolerable accuracy, although the restriction on the solution appears to be better than L curve criterion, a conclusion similar to one found previously [15]. The current approach indicates an alternative way to handle experimental data in the positron annihilation process.

ACKNOWLEDGMENTS

This work was supported by CNPq and FAPEMIG.

References

1. Mogensen, O. E. Positron Annihilation in Chemistry; Springer Verlag: Heidelberg, 1995.
2. Schrader, D. M.; Jean, Y. C. Positron and Positronium Chemistry Studies in Theoretical Chemistry; Elsevier: Oxford, 1988.
3. Courant, R.; Hilbert, D. Methods of Mathematical Physics; John Wiley, New York, 1989.
4. Hansen, P. C. Rank-Deficient and Discret Ill-Posed Problem, SIAM, Philadelphia, 1998.

5. Tikhonov, A. N.; Arsénine, V. *Méthods de Résolution de Problèmes Mal Posés*, Mir, Moscow, 1974.
6. Tikhonov, A. N.; Goncharsky, A. V. *Ill-Posed Problem in Natural Sciences*, Mir, Moscow, 1987.
7. Golub, G. H.; Van Loan, C. F. *Matrix Computations*, John Hopkins University Press, Baltimore, 1989.
8. Vemuri, V.; Jang, G. S. Inversion of Fredholm integral equation of first kind with fully connected neural networks. *J Franklin Inst* 1992, 329, 241.
9. Lemes, N. H. T.; Braga, J. P.; Belchior, J. C. Spherical potential energy function from second virial coefficient using Tikhonov regularization and truncated singular value decomposition. *Chem Phys Lett* 1998, 296, 233.
10. Braga, J. P.; Neves, J. L. Long-range spherical potential energy function from the second virial coefficient using decomposition into subspaces. *Phys Chem Chem Phys* 2001, 3, 4355.
11. Viterbo, V. C.; Braga, J. P.; Braga, A. P.; de Almeida, M. B. Inversion of simulated positron annihilation lifetime spectrum using a neural network. *J Chem Inf Comput Sci* 2001, 41, 309.
12. Forsythe, G. E.; Malcolm, M. A.; Moler, C. B. *Computer methods for mathematical computations*, Prentice-Hall, Inc., New Jersey, 1977.
13. Gregory, R. B.; Procyk, A. In Sharma, S. C., Ed. *International Symposium on Positron Annihilation Studies of Fluids*; World Scientific: Arlington, 1987; p. 524.
14. Bertero, M.; Boccacci, P. *Inverse Problems in Imaging*, IOP Publishing, Bristol, 1998.
15. Braga, J. P. Numerical comparison between Tikhonov regularization and singular value decomposition methods using the L curve criterion. *J Math Chem* 2001, 29, 151.